



Published in final edited form as:

*J Surg Res.* 2012 December ; 178(2): e43–e50. doi:10.1016/j.jss.2012.05.014.

## Bone Flap Perfusion Assessment using Near-Infrared Fluorescence Imaging

John T. Nguyen, M.D.<sup>1</sup>, Yoshitomo Ashitate, M.D.<sup>2</sup>, Ian A. Buchanan, B.A.<sup>1</sup>, Ahmed M.S. Ibrahim, M.D.<sup>1</sup>, Sylvain Gioux, Ph.D.<sup>3</sup>, Priti P. Patel, M.D.<sup>1</sup>, John V. Frangioni, M.D. Ph.D.<sup>3,4</sup>, and Bernard T. Lee, M.D., M.B.A.<sup>1</sup>

<sup>1</sup>Division of Plastic Surgery, Department of Surgery, Beth Israel Deaconess Medical Center, Boston, MA

<sup>2</sup>Division of Cancer Diagnostics and Therapeutics Hokkaido University Graduate School of Medicine, Sapporo, Japan

<sup>3</sup>Division of Hematology/Oncology, Department of Medicine, Beth Israel Deaconess Medical Center, Boston, MA

<sup>4</sup>Department of Radiology, Beth Israel Deaconess Medical Center, Boston, MA

### Abstract

**Background**—Microsurgical vascularized bone flaps are a versatile technique for reconstructing large bone defects. However, assessment of perfusion is challenging, as clinical examination is difficult intra-operatively and often not possible post-operatively. Therefore, it is important to develop techniques to assess perfusion of vascularized bone flaps, and potentially improve surgical outcomes. Near-infrared (NIR) fluorescence imaging has been previously shown to provide real-time, intra-operative evaluation of vascular perfusion. This pilot study investigates the ability of NIR imaging to assess perfusion of vascularized bone flaps.

**Materials and Methods**—Vascularized bone flaps were created on female Yorkshire pigs using well-established models for porcine forelimb osteomyocutaneous flap allotransplantation (N = 8) and hindlimb fibula flaps (N = 8). Imaging of the bone flaps was performed during harvest using the FLARE™ intraoperative fluorescence imaging system following systemic injection of indocyanine green (ICG). Perfusion was also assessed using standard of care by clinical observation and Doppler. NIR fluorescence perfusion assessment was confirmed by intermittent clamping of the vascular pedicle.

**Results**—NIR fluorescence imaging can identify bone perfusion at the cut end of the osteotomy site. When the vascular pedicle is clamped or ligated, NIR imaging demonstrates no fluorescence when injected with ICG. With clamp removal, the osteotomy site emits fluorescence indicating

© 2012 Elsevier Inc. All rights reserved.

Corresponding Author: Bernard T. Lee, MD, MBA, Beth Israel Deaconess Medical Center, Harvard Medical School, 110 Francis St. Suite 5A, Boston, MA 02215, Tel: 617-632-7835, Fax: 617-632-7840, blee3@bidmc.harvard.edu.

#### Financial Disclosure:

All FLARE™ technology is owned by Beth Israel Deaconess Medical Center, a teaching hospital of Harvard Medical School. As inventor, Dr. Frangioni may someday receive royalties if products are commercialized. Dr. Frangioni is the founder and unpaid director of The FLARE Foundation, a nonprofit organization focused on promoting the dissemination of medical imaging technology for research and clinical use.

**Publisher's Disclaimer:** This is a PDF file of an unedited manuscript that has been accepted for publication. As a service to our customers we are providing this early version of the manuscript. The manuscript will undergo copyediting, typesetting, and review of the resulting proof before it is published in its final citable form. Please note that during the production process errors may be discovered which could affect the content, and all legal disclaimers that apply to the journal pertain.

bone perfusion. Results using fluorescence imaging show 100% agreement with clinical observation and Doppler.

**Conclusion**—Vascularized bone transfers have become an important tool in reconstructive surgery; however, no established techniques adequately assess perfusion. Our pilot study indicates that NIR imaging can provide real-time, intra-operative assessment of bone perfusion.

### Keywords

Near-infrared imaging; vascularized bone flaps; bone perfusion; microsurgery; free flap; composite tissue allotransplantation

## INTRODUCTION

Vascularized bone flaps are used in reconstructive surgery for head and neck reconstruction, extremity reconstruction, and reconstruction of any large bony defect. These defects can result from postoncologic resections, trauma, infection, and congenital defects. The most common use of vascularized bone flaps is in oromandibular reconstruction for defects created by resection of oral cavity neoplasms or osteoradionecrosis of the mandible following radiation therapy [1–4]. These bony and soft tissue defects are complex and reconstruction often requires 3-dimensional composite tissue transfers for preservation of form and function. Microvascular reconstruction continues to be the standard of care for complicated mandibular reconstruction, and the most commonly used free flaps include the fibula, radial forearm, and iliac crest.

Early peri-operative monitoring of microsurgical flaps is critical to improve success rates [5–13]. Estimates in the literature of total flap loss after head and neck reconstruction are as high as 14%, with complication rates of 21% to 43% [1–13]. Composite tissue flaps that include vascularized bone grafts require optimal conditions to survive in biological settings. Preservation of a nutrient blood supply imparts viable osteoblasts and osteocytes, enabling primary healing of the graft to the recipient bone. Failure of vascularized bone grafts result in nonunion, fracture, and bone atrophy.

Monitoring of bone flaps is particularly challenging. After the inset of the bone segment and post-operatively, there is lack of direct access to the bony segment, which is buried. Standard methods of monitoring are limited because the ability to assess capillary refill and tissue color are not primary options on a bony flap. Attempts to circumvent this issue have centered on harvesting a monitoring flap such as an island cutaneous flap perfused by the same vessels as the buried components, but even in this setting flap loss rates remain high. Intra-operatively, prior to the inset of the bone segment, difficulties arise with determining the extent of perfusion of the harvested bone segment. Clinical evaluation is often inadequate for assessing the perfusion of the bone segment leaving to question the viability of the harvested bone. Currently, there are no adequate methods of assessment of intra-operative perfusion of bone flaps other than clinical observation of bleeding at the osteotomy sites after elevation and transfer [14]. Methods such as hand-held Doppler for perforator identification and postoperative monitoring can be highly operator dependent and unreliable. Limitations of Doppler use include interference from neighboring vessels, and the ability to only measure changes close to the surface [15].

Overall, the ability to rapidly assess microvascular compromise can significantly improve flap salvage and more efficacious methods are required for monitoring buried flaps both in the intra-operative and post-operative period. Disa et al. compared the salvage rate and final outcomes of buried versus nonburied flaps monitored by conventional techniques [16]. They

found that the overall free flap success rate was significantly lower for buried free flaps mainly due to delay in identifying flap failure.

Our group has previously described the Fluorescence-Assisted Resection and Exploration (FLARE™) near-infrared (NIR) imaging system and its potential for intraoperative surgical guidance [17–24]. This technology permits imaging in real-time, and in a safe, non-contact manner using a fluorescent probe capable of highlighting subsurface structures such as vasculature [17–20] or sentinel lymph nodes [25]. Fluorescent probes in the NIR range of 700 to 900 nm, such as indocyanine green (ICG), are usually preferred because NIR light can penetrate several millimeters into living tissue, offering excellent sensitivity to elicit fluorescence during angiography [18]. Consequently, NIR fluorescence imaging offers a sensitive and reliable method for monitoring tissue perfusion. The FLARE™ imaging system also has the capability of displaying merged images of NIR fluorescence with surgical anatomy at high resolution and in real time [23]. These digital images can be viewed in real time, and reviewed to determine optimal vessel choice during reconstructive operations. We describe our initial experience with NIR fluorescence imaging for intraoperative monitoring of perfusion in a pilot study of porcine osteomyocutaneous free flaps and vascularized bone flaps.

## MATERIALS AND METHODS

### Animals

Animal studies were performed under the supervision of Beth Israel Deaconess Medical Center's Institutional Animal Care and Use Committee (IACUC) in accordance with approved institutional protocol #155-2008. Female 35-kg Yorkshire pigs (E. M. Parsons and Sons, Hadley, MA) were used in this study. The pigs were induced with 4.4-mg/kg intramuscular Telazol (Fort Dodge Animal Health, Fort Dodge, IA), intubated, and maintained with 2% isoflurane (Baxter Healthcare Corp., Deerfield, IL). Physiological parameters (electrocardiography, heart rate, oxygen saturation, and body temperature) were monitored during all experiments. All animals included in this study were healthy with no prior history of allosensitization. A 14-gauge central venous catheter was inserted in the femoral vein prior to surgery.

### Anesthesia

On the day of the surgery, the animals were first premedicated with xylazine (Rompun®, 2 mg/kg) and ketamine hydrochloride (Ketaset®, 20 mg/kg). Thiopental sodium (Pentothal®, 50 mg) and atropine (0.5 mg) were then administered. The pigs were intubated and consequently connected to a Quantiflex ventilator (Matrix Medical, Inc., Orchard Park, NY). They were maintained on anesthesia throughout the procedure using 2% isoflurane (IsoFlot) in oxygen.

### NIR Fluorescence Imaging

The light source and optics of the current FLARE™ imaging system are attached to an articulated arm, which allows for positioning in 3-dimensional space while maintaining a working distance of 18 inches between the optics and the surgical field [17–24]. A light-guide coupled RF plasma light source generates > 40,000 lx of white light (400 to 650 nm), and a fiber coupled laser-diode source  $\approx 10$  mW/cm<sup>2</sup> of 760-nm NIR fluorescence provides excitation light over an area of 15 × 11 cm [26]. Color and NIR fluorescence images of the surgical field are acquired simultaneously via custom-designed optics and software [20]. ICG (1.25 mg; 36 µg/kg) was injected as a rapid bolus in 10 cc of saline.

## Surgical Procedure

**Forelimb Flap**—The pig radial forelimb composite tissue allotransplantation (CTA) flap is an osteomyocutaneous free flap based on the cephalic vein and brachial artery [27–32]. The flap consists of skin, muscle, bone, vessels and nerves, all of which are continuous with the medial digit. The vascular territories of the skin paddle were defined in the pig forelimb in our study by injecting ICG and performing NIR imaging. Once the location of the vessels was identified, an 8 × 8-cm paddle of skin was designed on the anteromedial aspect of the pig's forelimb approximately 3 cm below the elbow joint. As described previously [27–32], the cephalic vein was identified and dissected proximally.

The flexor carpi radialis was detached from its insertion on the medial epicondyle, and the brachial artery, medial and radial nerves were identified and dissected. Proximal and distal osteotomies were performed on the radius, and a vascularized 6-cm segment of radial bone was isolated. The neurovascular bundle supplying the radial forelimb osteomyocutaneous flap was left intact.

**Fibula Flap**—To elevate the vascularized fibula bone flap, an incision was made from the stifle (knee) joint parallel to the peroneal muscles on the lateral aspect of the hind limb to the tarsocrural joint [33–35]. After dividing the peroneus brevis and longus muscles in a longitudinal manner, the fibula was identified. The interosseous membrane (behind which the caudal tibial artery is located) was identified after dividing the insertions of the extensor digitorum and tibialis anterior muscles on the anterior aspect of the fibula. To avoid injuring the caudal tibial artery, the two perforating branches and vena comitantes were identified at their point of entry to the fibula, at which point the interosseous membrane was carefully stripped using a blade. This left a lengthy, fine slip of tibial periosteum close to the insertion of the membrane, at which point the flexor hallucis longus muscle was dissected posterolaterally. The fibula was then disarticulated using a gigli saw superiorly at the stifle and inferiorly at the tarsocrural joint.

## RESULTS

### Forelimb Flap

ICG was initially injected systemically to map out the location and distribution of arterial perforators to aid in the design of our skin flap. An 8 × 8 cm region was mapped out based on a perforator located on the forelimb of the pigs (Figure 1). Each composite tissue flap was elevated based on the cephalic vein and brachial artery. Following a second systemic ICG injection, the perfusion of each individual component (skin, muscle, bone) of our composite flap was visualized. Our skin paddle displayed a major perforator, with systemic ICG injection leading to progressive illumination of skin, muscle and bone segments (Figure 2). The bone segments of our composite tissue flap demonstrate perfusion at their distal ends clinically with bleeding at the osteotomy site. In addition, perfusion was assessed with a hand-held Doppler with 100% correlation.

Bone perfusion was further illustrated with clamping of the arterial vascular pedicle (Figure 3). Initially, the pedicle was clamped before ICG injection. The clamp was then released approximately 20 s after ICG injection with resulting perfusion of the isolated composite flap. The distal end of the bone segment progressively increased in fluorescence intensity indicating perfusion at the osteotomy site (Figure 3, right panel). These results demonstrate that NIR fluorescence imaging adequately confirms bone perfusion by the vascular pedicle. Arterial and venous clamping correlated with the clinical examination of skin color, turgor and capillary refill in the skin flap as well as bleeding at the osteotomy site. Hand-held

Doppler confirmed complete occlusion of the vessels with 100% correlation with the NIR imaging findings.

### Fibula flap

The fibula bone flap was harvested without a skin paddle. The interosseous membrane was identified and the vascular pedicle preserved prior to osteotomy. Systemic ICG injection was then performed as bone perfusion can be visualized within our fibular flap with NIR fluorescence at the distal end. This correlated with clinical findings of bleeding at the cut bone edge.

Comparison of a devascularized bone flap (where the pedicle was ligated) and a vascularized bone flap with NIR imaging shows corresponding NIR fluorescence at the osteotomy site in the vascularized flap with a lack of fluorescence in the devascularized flap (Figure 4). The devascularized bone showed no clinical perfusion or bleeding at the osteotomy site and the hand-held Doppler confirmed lack of flow in the pedicle. Finally, the vascularized bone flap showed bleeding at the bone edge and Doppler confirmation of perfusion at the vascular pedicle. We used signal-to-background ratio (SBR) for quantitation of fluorescence intensity (FI). SBR was calculated as follows; FI of region of interest (ROI) / FI of background (BG). The perforator (bone marrow) and the corner of the image were used as ROI and BG respectively. Vascularized bone marrow and devascularized bone marrow showed SBR=2.30 and 1.03, respectively.

## DISCUSSION

Presently, there exist no established techniques to effectively monitor the viability of vascularized bone grafts. In this pilot study, we were able to demonstrate that NIR fluorescence imaging has the ability to assess perfusion and viability of vascularized bone flaps. This was shown in two different anatomic locations and vascularized bone flap models: the osteomyocutaneous forelimb flap and the fibula flap. NIR fluorescence imaging was able to identify perfusion at both the osteotomy site and the vascular pedicle after flap elevation and harvest.

Recently, the perfusion of composite tissue flaps has been evaluated with the use of contrast angiography. [36,37] In addition, near-infrared angiography with ICG has been translated for clinical use with multiple applications in plastic surgery. [23,25,26,36] The end result is the ability to aid in the design and assessment of flap perfusion in the intra-operative period. [26,36] The study described here builds upon this body of work as we now describe the use of near infrared imaging to assess bony perfusion for the first time.

There are significant advantages in the use of NIR fluorescence imaging for vascularized bone flaps. First, NIR fluorescence imaging can be used to assist in flap design by locating perforator vessels. In the osteomyocutaneous composite forelimb flap, this allows us to create an 8 × 8 cm skin paddle based on an arterial perforator. Second, after flap elevation and harvest, including osteotomy, NIR imaging can demonstrate perfusion at the cut bone edges. As clinical examination of the bone flap is often difficult, this allows the reconstructive surgeon to identify that the bone flap is adequately vascularized. Clamping of the arterial pedicle in this study, with subsequent release was able to provide direct correlation between NIR imaging, clinical findings, and hand-held Doppler.

Another advantage to NIR fluorescence imaging is the possibility to directly assess bone perfusion at the vascular pedicle. This feature allows the surgeon to better assess the viability of the flap, and identify the origins of vascular compromise as well as devise a strategy intraoperatively. In clinical terms, assessing bone perfusion immediately after

harvest will allow the surgeon to make crucial decisions and actively intervene if necessary. Assessing bone perfusion immediately after microsurgical transfer will also allow the surgeon to make decisions about real-time perfusion abnormalities including spasm, thrombosis, or technical failure in anastomosis. This additional information can potentially influence changes in management, thus improving flap salvage and decreasing flap failure.

This technology however is limited once the bone segment is set into the reconstructed defect. The use of NIR imaging is therefore potentially an important adjunct in the intraoperative setting for evaluating bone perfusion. Once the bone is inset and plated, the ability to monitor perfusion in a composite flap is limited to the surface skin paddle. Thus, at this time our technology does not afford the ability to eliminate other commonly used post-operative flap monitoring methods. Contrast-enhanced high resolution ultrasound (hrCEUS) has recently been described to assess microcirculation of reconstructed bony defects; this technology may potentially allow assessment of perfusion post-operatively. [38] Once again, however, this is not an effective monitoring technique, as hrCEUS is not a continuous imaging device.

Another limitation of this technology is the slow and incomplete clearance of ICG within the time of surgery. ICG is a safe and widely used fluorophore that is FDA approved. With systemic injection of ICG, fluorescence is quickly seen (approximately 20 seconds) at the distal end of our osteotomy site after the initial injection. This fluorescence persists after the injection with a decrease in intensity to 50% after approximately 10 minutes. After 30 minutes, the ICG has washed out to a level that is approximately 15% of its peak intensity, but after 60 minutes the fluorescence levels return to baseline. Therefore the time needed for a complete fluorescent washout would be approximately 60 min. By measuring the intensity of our fluorescence over time, which was described in our previous papers [39], we have determined the time required for the ICG to washout. We have found that ICG can be infused approximately every ten minutes and repeated up to five times before the ability to discern details such as vasculature is lost due to residual fluorescence. Newer fluorescent dyes are currently being designed for faster clearance, therefore reducing the background contamination [40]. Although this pilot study describes our initial work with near infrared imaging of bony perfusion, we are currently working on developing quantitative metrics to assess flap perfusion and vascular compromise. This will allow us to develop quantitative analysis similar to what has previously been described from our laboratory using this technology in other flap models [39].

NIR fluorescence imaging has shown to be a promising tool to provide surgeons with feedback in real-time during surgery. This imaging modality has successfully been used during first-in-human trials for sentinel lymph node mapping [25] and breast reconstruction following mastectomy [23]. In this study, fluorescence imaging was successfully validated in porcine models to assess perfusion of vascularized bone flaps. Overall, this emergent technology shows promise in its ability to monitor bone perfusion peri-operatively and could therefore allow the surgeon to intervene and improve outcomes. This may someday prove valuable to the reconstruction of large bone defects.

## Acknowledgments

### Sources of Funding:

This study was funded by National Institutes of Health grants #R01-CA-115296 (National Cancer Institute) and #R01-EB-005805 (National Institute of Biomedical Imaging and Bioengineering) to JVF.



## References

1. Hirsch DL, Bell RB, Dierks EJ, et al. Analysis of microvascular free flaps for reconstruction of advanced mandibular osteoradionecrosis: a retrospective cohort study. *J Oral Maxillofac Surg.* 2008; 66:2545–56. [PubMed: 19022135]
2. Smeele LE, Goldstein D, Tsai V, et al. Morbidity and cost differences between free flap reconstruction and pedicled flap reconstruction in oral and oropharyngeal cancer: Matched control study. *J Otolaryngol.* 2006; 35(2):102–7. [PubMed: 16527028]
3. de Bree R, Reith R, Quak JJ, et al. Free radial forearm flap versus pectoralis major myocutaneous flap reconstruction of oral and oropharyngeal defects: a cost analysis. *Clin Otolaryngol.* 2007; 32:275–82. [PubMed: 17651269]
4. Cannady SB, Dean N, Kroeker A, et al. Free flap reconstruction for osteoradionecrosis of the jaws--outcomes and predictive factors for success. *Head Neck.* 2011; 33:424–8. [PubMed: 20645290]
5. Wei FC, Demirkan F, Chen HC, et al. The outcome of failed free flaps in head and neck and extremity reconstruction: what is next in the reconstructive ladder? *Plast Reconstr Surg.* 2001; 108:1154–60. [PubMed: 11604611]
6. Jones NF, Jarrahy R, Song JJ, et al. Postoperative medical complications - not microsurgical complications - negatively influence the morbidity, mortality, and true costs after microsurgical reconstruction for head and neck cancer. *Plast Reconstr Surg.* 2007; 119:2053–60. [PubMed: 17519700]
7. Bui DT, Cordeiro PG, Hu QY, et al. Free flap reexploration: indication, treatment, and outcomes in 1193 free flap. *Plast Reconstr Surg.* 2007; 119:2092–2100. [PubMed: 17519706]
8. Brown JS, Devine JC, Magennis P, et al. Factors that influence the outcome of salvage in free tissue transfer. *Br J Oral Maxillofac Surg.* 2003; 41:16–20. [PubMed: 12576035]
9. Khouri RK, Cooley BC, Kunselman AT, et al. A prospective study of microvascular free-flap surgery and outcome. *Plast Reconstr Surg.* 1008; 102:711–721. [PubMed: 9727436]
10. Kroll SS, Schusterman MA, Reece GP, et al. Timing of pedicle thrombosis and flap loss after free-tissue transfer. *Plast Reconstr Surg.* 1996; 98:1230–1233. [PubMed: 8942909]
11. Smit JM, Acosta R, Zeebregts CJ, et al. Early reintervention of compromised free flaps improves success rate. *Microsurgery.* 2007; 27:612–616. [PubMed: 17868141]
12. Rozen WM, Chubb D, Whitaker IS, Acosta R. The efficacy of postoperative monitoring: a single surgeon comparison of clinical monitoring and the implantable Doppler probe in 547 consecutive free flaps. *Microsurgery.* 2010; 30:105–110. [PubMed: 19790183]
13. Lin SJ, Nguyen MD, Chen C, Colakoglu S, Curtis MS, Tobias AM, Lee BT. Tissue oximetry monitoring in microsurgical breast reconstruction decreases flap loss and improves rate of flap salvage. *Plast Reconstr Surg.* 2011; 127(3):1080–1085. [PubMed: 21364410]
14. Jallali N, Ridha H, Butler PE. Postoperative monitoring of free flaps in UK plastic surgery units. *Microsurgery.* 2005; 25:469–72. [PubMed: 16134095]
15. Hallock GG. Doppler sonography and color duplex imaging for planning a perforator flap. *Clin Plast Surg.* 2003; 30:347–357. v–vi. [PubMed: 12916592]
16. Disa JJ, Cordeiro PG, Hidalgo DA. Efficacy of conventional monitoring techniques in free tissue transfer: an 11-year experience in 750 consecutive cases. *Plast Reconstr Surg.* 1999; 104:97–101. [PubMed: 10597680]
17. Matsui A, Lee BT, Winer JH, et al. Image-guided perforator flap design using invisible near-infrared light and validation with x-ray angiography. *Ann Plast Surg.* 2009; 63:327–330. [PubMed: 19692894]
18. Matsui A, Lee BT, Winer JH, et al. Submental perforator flap design with a near-infrared fluorescence imaging system: the relationship among number of perforators, flap perfusion, and venous drainage. *Plast Reconstr Surg.* 2009; 124:1098–1104. [PubMed: 19935293]
19. Matsui A, Lee BT, Winer JH, et al. Quantitative assessment of perfusion and vascular compromise in perforator flaps using a near-infrared fluorescence-guided imaging system. *Plast Reconstr Surg.* 2009; 124:451–460. [PubMed: 19644259]

20. Matsui A, Lee BT, Winer JH, et al. Predictive capability of near-infrared fluorescence angiography in submental perforator flap survival. *Plast Reconstr Surg.* 2010; 126:1518–1527. [PubMed: 21042109]
21. Matsui A, Lee BT, Winer JH, et al. Real-time intraoperative near-infrared fluorescence angiography for perforator identification and flap design. *Plast Reconstr Surg.* 2009; 123:125e–127e.
22. Lee BT, Matsui A, Hutteman M, et al. Intraoperative near-infrared fluorescence imaging in perforator flap reconstruction: current research and early clinical experience. *J Reconstr Microsurg.* 2010; 26:59–65. [PubMed: 20027541]
23. Lee BT, Hutteman M, Gioux S, et al. The FLARE intraoperative near-infrared fluorescence imaging system: a first-in-human clinical trial in perforator flap breast reconstruction. *Plast Reconstr Surg.* 2010; 126:1472–1481. [PubMed: 21042103]
24. Tanaka E, Chen FY, Flaumenhaft R, et al. Real-time assessment of cardiac perfusion, coronary angiography, and acute intravascular thrombi using dual-channel near-infrared fluorescence imaging. *J Thorac Cardiovasc Surg.* 2009; 138:133–140. [PubMed: 19577070]
25. Gioux S, Kianzad V, Ciocan R, et al. High-power, computer-controlled, light-emitting diode-based light sources for fluorescence imaging and image-guided surgery. *Mol Imaging.* 2009; 8:156–165. [PubMed: 19723473]
26. Mieog JS, Troyan SL, Hutteman M, et al. Toward optimization of imaging system and lymphatic tracer for near-infrared fluorescent sentinel lymph node mapping in breast cancer. *Ann Surg Oncol.* 2011 Sep; 18(9):2483–91. [PubMed: 21360250]
27. Gioux S, Mazhar A, Lee BT, et al. First-in-human pilot study of a spatial frequency domain oxygenation imaging system. *J Biomed Opt.* 2011 Aug.16(8):086015. [PubMed: 21895327]
27. Kuo YR, Sacks JM, Lee WP, et al. Porcine heterotopic composite tissue allograft transplantation using a large animal model for preclinical studies. *Chang Gung Med J.* 2006; 29:268–74. [PubMed: 16924888]
28. Vossen M, Edelstein J, Majzoub RK, et al. Bone quality and healing in a swine vascularized bone allotransplantation model using cyclosporine-based immunosuppression therapy. *Plast Reconstr Surg.* 2005; 115:529–38. [PubMed: 15692359]
29. Ren X, Shirbacheh MV, Ustüner ET, et al. Osteomyocutaneous flap as a preclinical composite tissue allograft: swine model. *Microsurgery.* 2000; 20:143–9. [PubMed: 10790178]
30. Zdichavsky M, Jones JW, Ustuner ET, et al. Scoring of skin rejection in a swine composite tissue allograft model. *J Surg Res.* 1999; 85:1–8. [PubMed: 10383831]
31. Ustüner ET, Majzoub RK, Ren X, et al. Swine composite tissue allotransplant model for preclinical hand transplant studies. *Microsurgery.* 2000; 20:400–6. [PubMed: 11150991]
32. Ustüner ET, Zdichavsky M, Ren X, et al. Long-term composite tissue allograft survival in a porcine model with cyclosporine/mycophenolate mofetil therapy. *Transplantation.* 1999; 66:1581–7.
33. Gur E, Chiodo A, Pang CY, et al. The vascularized pig fibula bone flap model: effects of multiple segmental osteotomies on growth and viability. *Plast Reconstr Surg.* 1999; 103:1436–42. [PubMed: 10190440]
34. Chiodo AA, Gur E, Pang CY, et al. The vascularized pig fibula bone flap model: effect of segmental osteotomies and internal fixation on blood flow. *Plast Reconstr Surg.* 2000; 105:1004–12. [PubMed: 10724261]
35. Chiodo AA, Forrest CR, Pang CY, et al. Anatomic and hemodynamic study of the vascularized pig fibula bone flap model. *J Otolaryngol.* 1996; 25:103–7. [PubMed: 8683649]
36. Liu DZ, Mathes DW, Zenn MR, Neligan PC. The application of indocyanine green fluorescence angiography in plastic surgery. *J Reconstr Microsurg.* 2011; 27(6):355–64. [PubMed: 21717392]
37. Munding GS, Kelamis JA, Kim SH, et al. Tunneled superficial inferior epigastric artery (SIEA) myocutaneous/vascularized femur chimeric flaps: A model to study the role of vascularized bone marrow in composite allografts. *Microsurgery.* 2012; 32(2):128–35. [PubMed: 22113953]
38. Prantl L, Pfeifer C, Geis S, et al. Osteocutaneous free flaps: a critical analysis of quantitative evaluation of bone microcirculation with contrast-enhanced high resolution ultrasound (hrCEUS) and TIC analysis. *Clin Hemorheol Microcirc.* 2011; 49(1–4):251–9. [PubMed: 22214696]



39. Ashitate Y, Lee BT, Ngo LH, et al. Quantitative assessment of nipple perfusion with near-infrared fluorescence. imaging. *Ann Plast Surg.* 2011 Aug 22. [epub ahead of print].
40. Choi HS, Nasr K, Alyabyev S, et al. Chem synthesis and in vivo fate of zwitterionic near-infrared fluorophores. *Int Ed Engl.* 2011; 50(28):6258–63.

\$watermark-text

\$watermark-text

\$watermark-text

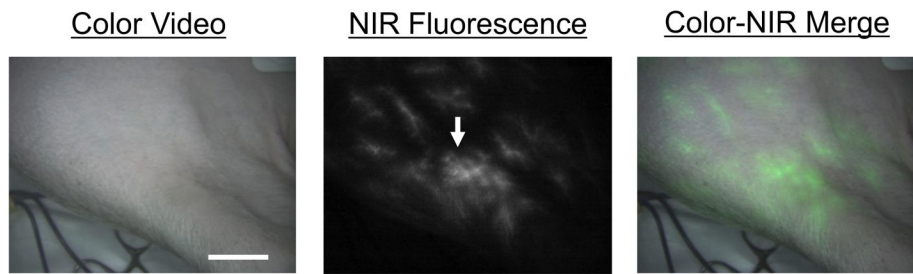


**Figure 1.** Forelimb composite flap design using NIR fluorescence imaging. The imaging system shows the surgical field in color (left), NIR fluorescence (middle), and a merged image of the two (right). After injection of ICG, the cutaneous perforators can be identified (arrow). Scale bar = 3 cm.

\$watermark-text

\$watermark-text

\$watermark-text

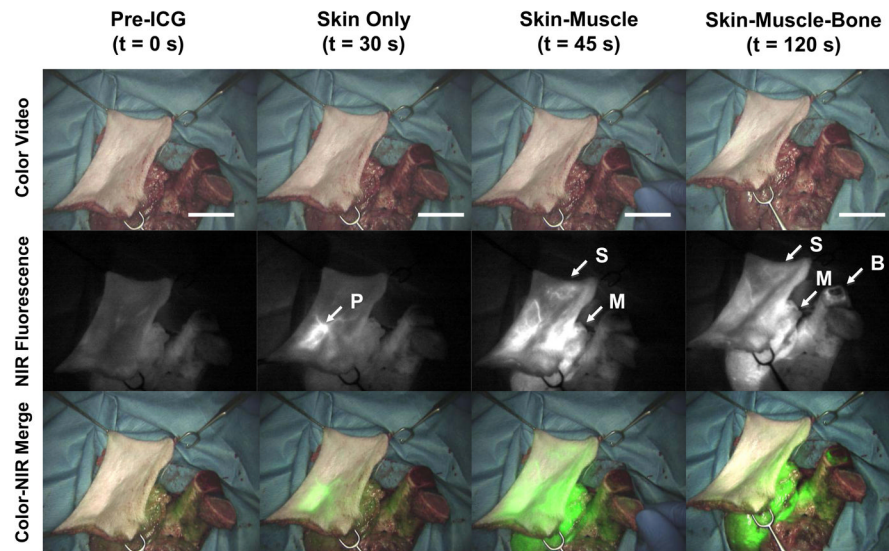


**Figure 2.** Forelimb composite flap showing progressive perfusion of skin, muscle and bone. Prior to ICG injection, there is no NIR fluorescence signal (left column). After ICG injection, at 30 s the skin perforator shows fluorescence (left middle column, arrow labeled P depicts skin perforator), at 45 s the skin paddle is further perfused as well as the muscle (right middle column, arrow labeled S depicts peripheral skin, arrow labeled M depicts muscle), at 120 s the cut end of the bone is perfused (right column; arrow labeled B depicts bone perfusion). Scale bar = 3 cm.

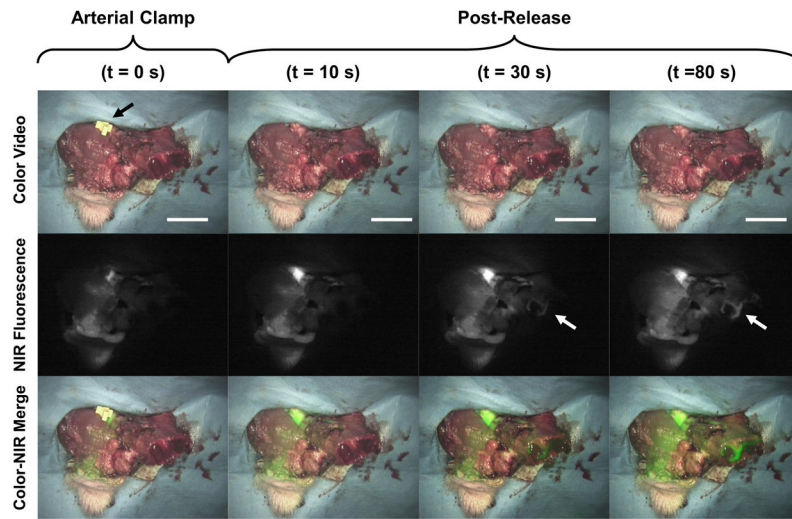


**Figure 3.** Forelimb composite flap during arterial clamping. ICG is injected while the artery is clamped (left column). After release of the arterial clamp there is progressive perfusion of the skin, muscle, and bone (arrow depicts bone perfusion). Scale bar = 3 cm.

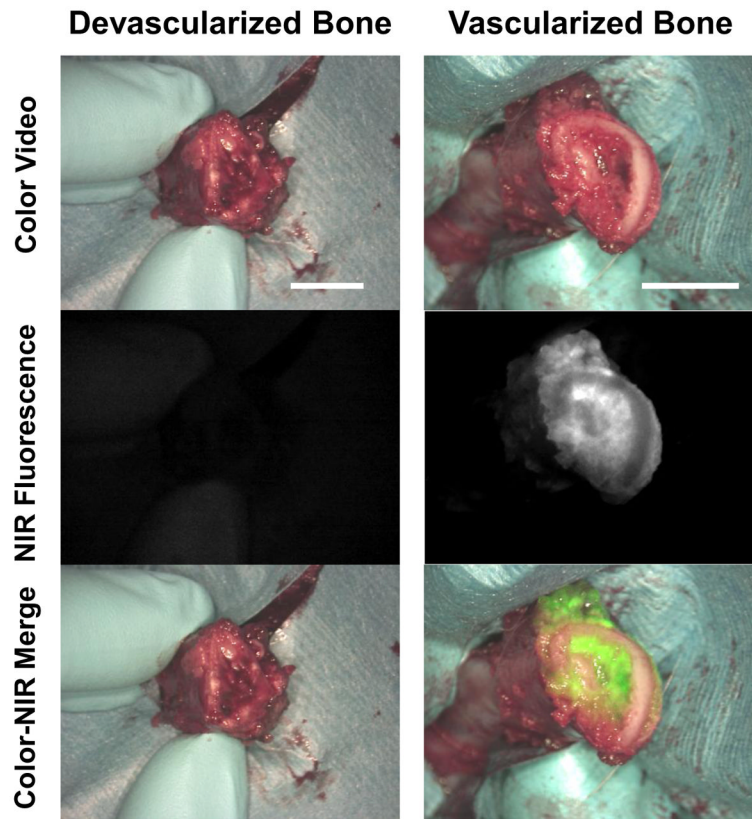


**Figure 4.** Fibula flap with a devascularized, ligated pedicle (left column) shows no perfusion or NIR fluorescence. Fibula flap with a vascularized pedicle (right column) shows NIR perfusion of the osteotomy site and cut bone edges. Scale bar = 1 cm.